Journal of Hazardous Materials, Volume 431, June 2022, Article number 128530
DOI:10.1016/j.jhazmat.2022.128530

Impact of Resin Loading on Ion Exchange Equilibrium for Removal of Organic Matter and Inorganic Ions

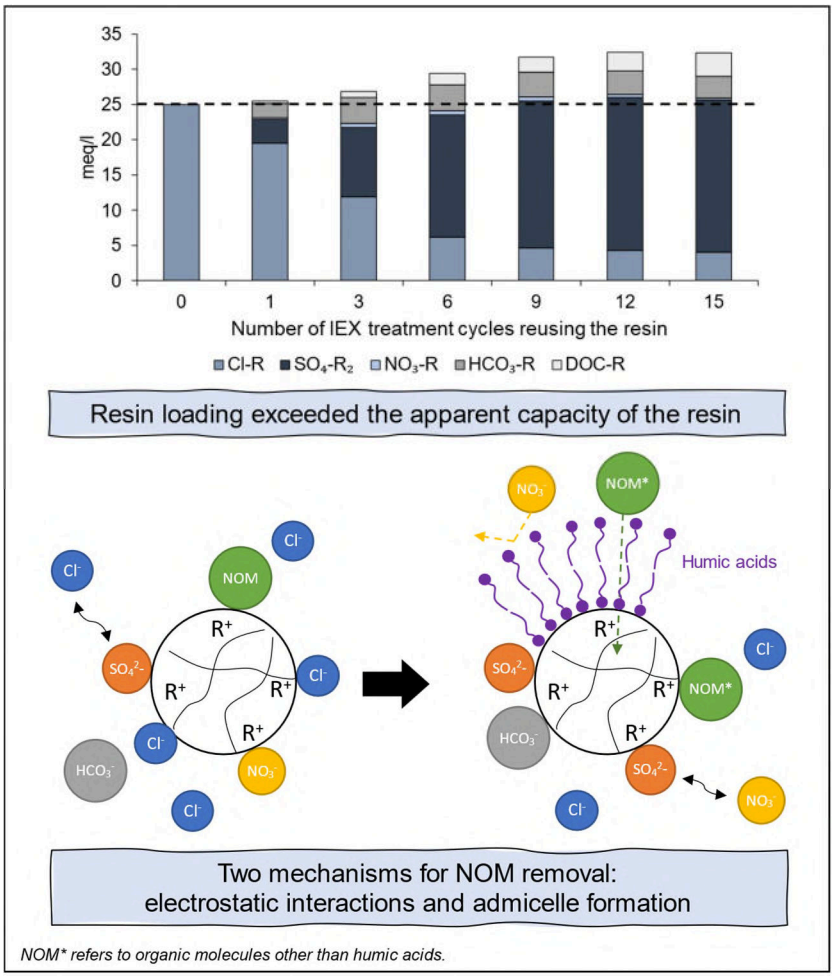
Lucie Pidoux[a], Holly Shorney-Darby[b], Elisabeth Vaudevire[b], Bram Martijn[b], Peter Jarvis[a], Irene Carra[a*]

[a]Cranfield Water Science Institute, Building 52a, Cranfield University, Cranfield, MK43 0AL, UK

[b]PWN Technologies R&D, Dijkweg 1, 1619 HA P.O. Box 66, Andijk 1619 ZH, The Netherlands

*corresponding author email: irene.carra@cranfield.ac.uk

GRAPHICAL ABSTRACT



ABSTRACT

Ion Exchange (IEX) applications for drinking water can be limited due to high volumes of brine, brine waste and treated water corrosivity. Reusing the resin by operating at reduced regeneration frequency can overcome this. However, assessing changes on the resin loading over reuse cycles is complex because multiple presaturant ions participate in the exchange and existing models only account for the exchange with one presaturant ion. This study developed a theoretical multicomponent model for the determination of IEX equilibria when the resin loading increases due to reuse. The model suggested that both electrostatic interactions and admicelle formation were the separation mechanisms. The model revealed that under reduced regeneration frequencies, brine use and waste generation can be reduced by more than 90%, where the bicarbonate-form resin offered the potential for lower corrosivity. However, changes in resin loading after 5 reuse cycles showed that the risk of corrosion increased. For the tested source water, reusing the bicarbonate-form resin every 5 cycles would achieve the most sustainable option with 41% NOM removal and 79% brine and waste reduction. Under these conditions, almost 100% of exchange capacity is recovered after regeneration.

Keywords: adsorption; equilibrium; ion exchange; natural organic matter; selectivity

Published by Elsevier. This is the Author Accepted Manuscript issued with: Creative Commons Attribution Non-Commercial No Derivatives License (CC:BY:NC:ND 4.0). The final published version (version of record) is available online at DOI:10.1016/j.jhazmat.2022.128530. Please refer to any applicable publisher terms of use.

LIST OF ABBREVIATIONS

AC	Adsorption capacity
BV	Bed volume(s)
CSMR	Chloride to sulphate mass ratio
DI	Deionised water
DOC	Dissolved organic carbon
EC	Exchange capacity
IC	Ion chromatography
IEX	Ion exchange
LC-OCD	Liquid chromatography organic carbon detection
LR	Larson ratio
MIEX	Magnetic Ion Exchange
NOM	Natural organic matter
NPOC	Non-purgeable organic carbon
RV	Resin volume
SBA	Strong base anion
SIX	Suspended ion exchange
TOC	Total organic carbon

NOMENCLATURE

a	Activity
A	Presaturant ion
B	Counterion
K	Selectivity coefficient
R	Volume ratio of resin to liquid (L bulk resin/L solution)
γ_i	Activity coefficient
n	Valence
X^-	Monovalent ion
Y^{2-}	Divalent ion
$[i]_0$	Initial concentration of ion i (mol/L)
$[i]$	Concentration of ion i at equilibrium (mol/L)
$i-R$	Resin-phase ion

1 INTRODUCTION

Ion Exchange (IEX) has shown efficient natural organic matter (NOM) removal for drinking water production, from both hydrophobic and hydrophilic rich water sources. It can be used as a front barrier treatment for NOM, sometimes in combination with other processes such as coagulation or membranes (Carra et al., 2021; Fernandez 2021a; Finkbeiner et al., 2018). However, as it operates today, the resin requires regular regeneration (usually with NaCl) to avoid irreversible fouling, which results in large volumes of chloride brine and high amounts of waste. For example, in the Suspended Ion Exchange (SIX) process, the resin is operated in single-pass mode before regeneration (Semmens *et al.*, 2000; PWN Technologies, 2017).

In addition, the release of chloride during the IEX process increases the corrosivity of the treated water (Fernandez 2021a), generating potential issues with lead and discolouration in the distribution system (Nguyen *et al.*, 2011; Tang *et al.*, 2018). Previous research has shown that bicarbonate reduces the corrosivity of the treated water and has shown promising results at lab scale when used as an alternative regenerant (Rokicki and Boyer, 2011; Fernandez 2021b). Another potential way of reducing the treated water corrosivity is by decreasing the regeneration frequency of the IEX process (resin reuse), which would also allow for reductions in brine and waste volumes. However, assessing the impact of several reuse cycles on resin loading and process efficiency is challenging.

This is because of the complexity of IEX mechanisms. IEX occurs mainly through electrostatic interactions that consist in the exchange of an ion present in solution (counterion) with an ion equally charged and attached to a solid particle (presaturant ion). IEX equilibrium theory is commonly used to describe these interactions (Crittenden *et al.*, 2012; SenGupta, 2017) and can be applied to describe the behaviour of IEX processes. A wide range of models have been developed over the past 60 years to predict the composition of multicomponent systems at equilibrium. The majority of these models are based on the law of mass action and are frequently combined with adsorption isotherms (Dranoff and Lapidus, 1957; Boyer, Baird and Nirdosh, 1999; Hannachi, Guesmi and Hamrouni, 2013), where multicomponent systems are considered equivalent to a combination of independent binary systems

and ideality is assumed in both aqueous and resin phases. The research from Zhang *et al.* (2014) differs slightly from the others as it relies on polyparameter linear-free energy relationships.

Although these models have been promising, they commonly predict IEX equilibrium with a resin initially saturated with one single ion (i.e chloride). When the IEX resin is reused over more than one treatment cycle before regeneration, more than one ion will occupy the active sites of the resin. These ions become presaturant ions which may exchange with counterions in subsequent treatment cycles in secondary IEX (Fernandez et al., 2021b). The challenge is then to model this multiple exchange where not only chloride, but also other inorganic ions and NOM previously adsorbed on the resin can exchange with ions in the aqueous phase. The basis of the multiple exchange is based on the selectivity of each counterion towards the resin. Therefore, developing a model that accounts for changes in the resin loading over several reuse cycles would provide an understanding of the IEX equilibrium, and thus, NOM and inorganic ions removal, water quality and corrosivity at reduced regeneration frequency. Moreover, such a model will help identify the optimal operation of IEX treatment to achieve the required water quality whilst minimising brine and waste.

The novelty of this study resides in the development of a theoretical multicomponent model for the prediction of IEX equilibria of both NOM and inorganic ions with increasing resin loading. Firstly, the model was used to determine the selectivity coefficients of NOM and inorganic ions. Subsequently, the model was used to estimate the IEX equilibria and compared to experimental data. The applicability of the model was investigated by establishing the implications of reduced regeneration frequency on IEX capacity, corrosivity, brine use and waste production. River water from a lowland source in the UK was used for testing and chloride or bicarbonate were used as regenerants.

2 MATERIALS AND METHODS

2.1 Suspended IEX jar test data

To test the applicability of the model to predict IEX equilibria in a multicomponent system at increased resin loading, experimental data from 15 jar tests where the resin was reused without regeneration was used. The data was taken from the work of Fernandez et al. (2021b) and includes results for 15 consecutive suspended IEX jar tests using water from a lowland river in the UK with no resin regeneration (Table S1). Treatment time was 30 min, which is a typical retention time in large scale suspended IEX contactors and a point at which a pseudo-equilibrium is reached (Galjaard *et al.*, 2018). Further details on the experimental procedure can be found on Text S1. The resin used in this study was Lewatit® S 5128 (Lanxess, Germany), a gellular type I strong base anion (SBA) exchange resin with quarternary ammonium functional groups in an acrylic matrix. The resin is delivered in the chloride form and has an adsorption capacity (AC) of 1.25 eq/L_{resin} (Lenntech, 2016).

The Lewatit® S 5128 resin was initially saturated with chloride or bicarbonate and the subsequent jar tests were carried out without regeneration between treatment cycles. The ionic content of the lowland river water tested was as follows: DOC = 6.5 mg/L, [Cl^-] = 78.7 mg/L, [NO_3^-] = 36.7 mg/L, [SO_4^{2-}] = 171.1 mg/L, Alkalinity = 192.5 mg $CaCO_3$/L and pH = 8.2. Experiments were conducted with a resin dose of 20 mL_{resin}/L, resulting in an exchange capacity (EC) of 25 meq/L.

2.2 IEX Model

2.2.1 Determination of selectivity coefficients in a multicomponent system

Electrostatic, or coulombic, interaction between ions in solution and ions on the resin is the predominant mechanism taking place in an IEX process (SenGupta, 2017). These interactions lead to the replacement of one ion with another while preserving the electroneutrality of the system. Therefore, IEX is commonly expressed as a stochiometric process that allows for reversibility to occur (Crittenden *et al.*, 2012; SenGupta, 2017). For a base anion resin, the binary exchange reaction can be written as:

$$nA\text{-}R + B^{n-} \leftrightarrow B\text{-}R_n + nA^- \quad \textbf{(1)}$$

where A^- is the presaturant ion, B^{n-} is the counterion with valence of n and R^+ is the ionic group attached to the resin.

When the resin is placed in solution, an equilibrium state is reached between the ions in the solution and ions on the resin, and the distribution of species can be described applying the law of mass action (Crittenden *et al.*, 2012):

$$K_{B\backslash A} = \frac{{a_A}^n \, a_{B-R_n}}{{a_{A-R}}^n \, a_B} \quad \textbf{(2)}$$

Where a_A and a_B are the activities of presaturant ion A and counterion B in the aqueous-phase; and a_{A-R}, a_{B-R_n} are the activities of ions A and B in the resin-phase. $K_{B\backslash A}$ is the selectivity coefficient and illustrates the affinity of the counterion B for the resin presaturated with the anion A -the higher the value of $K_{B\backslash A}$, the higher the preference for the resin (Crittenden *et al.*, 2012).

By definition, the activity can be written as $a_i = \gamma_i . [i]$ where γ_i expresses the activity coefficient and $[i]$ the molar concentration of ion i at equilibrium (mol/L).

Therefore, equation (2) can be written as follows

$$K_{B\backslash A} = \frac{[A]^n \, [B - R_n]}{[A - R]^n \, [B]} \times \frac{{\gamma_A}^n}{{\gamma_{A-R}}^n} \times \frac{\gamma_{B-R_n}}{\gamma_B} \quad \textbf{(3)}$$

In water treatment, dilute electrolyte solutions where all the molecules interact identically are typically present and, as such, are treated as ideal solutions. In such context, the activities of the ions in solution tend towards the measured molar concentrations (i.e. γ_i=1) (Crittenden *et al.*, 2012). As of today, techniques to directly quantify the activities in the resin-phase are missing and the theoretical equilibrium approach commonly assumes ideal conditions in the exchanger too (i.e. γ_i=1) (SenGupta, 2017). Consequently, this simplification results in a new expression of the thermodynamic equilibrium constant $K_{B\backslash A}$, referred to as the selectivity coefficient:

$$K_{B\backslash A} = \frac{[A]^n\,[B - R_n]}{[A - R]^n\,[B]} \quad \textbf{(4)}$$

The selectivity coefficients of NOM and inorganic ions (sulphate, nitrate, chloride and bicarbonate) were calculated as part of a multicomponent system. This was done by applying the selectivity coefficient term (Eq. 4) to the equilibrium data obtained from the jar tests conducted in multicomponent systems (Table S1, cycle 1), similar to the approach of Liu *et al.* (2017). The molar concentrations of ion *i* in the resin-phase were estimated as follows:

$[i - R] = [i]_0 - [i]$

where $[i - R]$ refers to the concentration of counterion i adsorbed on resin

$[Cl - R] = [Cl - R]_0 - ([Cl^-] - [Cl^-]_0)$

where $[Cl - R]$ refers to the concentration of the presaturant ion Cl^- left on resin.

2.2.2 Determination of IEX equilibria

The model was developed to predict IEX equilibria with increasing resin loading due to the reuse of the resin without regeneration and is based on an adaption of the method developed by Boyer, Baird and Nirdosh (1999). The model was coded and applied to the experimental data in MATLAB (Text S2). It accounts for IEX equilibria when the resin is initially saturated with one single ion (either chloride or bicarbonate) and when more than one type of ion (either NOM, chloride, bicarbonate, sulphate or nitrate) occupies the resin active sites before the following cycle of IEX without regeneration. The following method is described for a monovalent and divalent ion (X^- and Y^{2-}) in equilibrium with the chloride-form resin as an example. An analogous code was used for the bicarbonate-form resin.

To predict the equilibrium after IEX with a resin initially saturated with one ion, the first step considered the mass balance for each solute and the electroneutrality at equilibrium:

$$[Cl^-] = [Cl^-]_0 + EC(1 - \alpha) \quad \textbf{(5)}$$

with $\alpha = \frac{[Cl-R]}{EC}$; 0 ≤ α ≤ 1 and $EC = AC \times R$ where R is the volume ratio of resin to liquid.

$$[Cl^-] = [Cl^-]_0 + [X^-]_0 + 2\,[Y^{2-}]_0 - [X^-] - 2\,[Y^{2-}] \quad \textbf{(6)}$$

$$[X - R] = [X^-]_0 - [X^-] \quad \textbf{(7)}$$

$$[Y - R_2] = [Y^{2-}]_0 - [Y^{2-}] \quad \textbf{(8)}$$

Using Eq. 4 and the equations above, $K_{X\backslash Cl}$ can be expressed as

$$K_{X\backslash Cl} = \frac{\left([Cl^-]_0 + EC(1-\alpha)\right)[X-R]}{[X^-]\;\alpha\;EC} \quad \textbf{(9)}$$

which leads to

$$[X^-] = \frac{[X^-]_0}{1 + \frac{K_{X\backslash Cl}\;\alpha\;\mathrm{EC}}{[Cl^-]_0 + \mathrm{EC}(1-\alpha)}} \quad \textbf{(10)}$$

Similarly, rearranging $K_{Y\backslash Cl}$ leads to

$$[Y^{2-}] = \frac{[Y^{2-}]_0}{1 + \frac{K_{Y\backslash Cl}\;(\alpha\mathrm{EC})^2}{\left([Cl^-]_0 + \mathrm{EC}(1-\alpha)\right)^2}} \quad \textbf{(11)}$$

Consequently, the four concentrations (Eq. 5, 6, 10 and 11) can be solved by iteration, varying α until the two expressions of $[Cl^-]$ match. In the present work, α has been given an initial value of zero and was increased by 10^{-8} at each iteration. The concentrations given by the model indicates the ionic content at equilibrium.

When the same resin was reused for consecutive IEX treatment cycles without regeneration, the resin became saturated with more than one ion. Therefore, at cycle j (j>1), the mass and charge balances become:

$$[Cl^-]_j = [Cl^-]_0 + [Cl-R]_{j-1} - \alpha_j\,EC \quad \textbf{(12)}$$

with $\alpha_j = \frac{[Cl-R]_j}{EC}$; 0 ≤ α_j ≤ 1.

$$[Cl^-]_j = [Cl^-]_0 + [X^-]_0 + 2\,[Y^{2-}]_0 - [X^-]_j - 2\,[Y^{2-}]_j \quad \textbf{(13)}$$

$$[X-R]_j = [X-R]_{j-1} + [X^-]_0 - [X^-]_j \quad \textbf{(14)}$$

$$[Y-R_2]_j = [Y-R_2]_{j-1} + [Y^{2-}]_0 - [Y^{2-}]_j \quad \textbf{(15)}$$

After rearranging $K_{X\backslash Cl}$ and $K_{Y\backslash Cl}$, the following equations are obtained:

$$[X^-]_j = \frac{[X^-]_0 + [X-R]_{j-1}}{1 + \dfrac{K_{X\backslash Cl}\;\alpha_j\;EC}{[Cl^-]_0 + [Cl-R]_{j-1} - \alpha_j\;EC}} \quad \textbf{(16)}$$

$$[Y^{2-}]_j = \frac{[Y^{2-}]_0 + [Y-R_2]_{j-1}}{2 + \dfrac{K_{Y\backslash Cl}\;(\alpha_j\;EC)^2}{\left([Cl^-]_0 + EC(1-\alpha_j)\right)^2}} \quad \textbf{(17)}$$

Similarly, at cycle j, equations 12, 13, 16 and 17 are iterated by varying α_j until the two expressions of $[Cl^-]_j$ match. Likewise, α_j has been given an initial value of zero and has been increased by 10^{-8} at each iteration.

2.2.3 Modelling of the resin regeneration

When the resin is used in a treatment cycle, the IEX sites become occupied by different contaminants. The regeneration of the resin involves exchange of those ions and replacing them with the original presaturant ion (either chloride or bicarbonate) so the exchanger can continue to be used. This is achieved by placing the exhausted resin in contact with a highly concentrated chloride or bicarbonate solution, while keeping the resin in suspension.

The equilibrium state can be approached similarly in the two directions of the chemical reaction (Crittenden *et al.*, 2012) since the concentration gradient is the driving force for the exchange to achieve equilibrium. Therefore, high concentrations of chloride or bicarbonate will drive the equilibrium and the regeneration reaction can be expressed as:

$$B - R_n + n\,A^- \;\leftrightarrow\; n\,A - R + B^{n-} \quad \textbf{(18)}$$

A single regeneration with a 1 M chloride or bicarbonate brine was considered here. In this study, the composition of the system after regeneration is given at steady state. The corresponding MATLAB script is reported in Supplementary Information (Text S3).

2.3 Brine use and waste production

The volumes of used brine and produced waste per day were estimated for a suspended IEX process, for a resin dose of 20 mL/L and contact time of 30 min (conditions as used in the lab jar tests). The brine and wastewater production were based on the operation as used in the commercially available SIX process. In this process the brine and rinse water volume are twice the resin volume each (Fernandez, 2021a).

2.4 Corrosivity indexes

The Larson Ratio (LR) and the chloride to sulphate mass ratio (CSMR) were used to assess the corrosivity of the treated water at reduced regeneration frequency. High LR values indicate a risk of corrosion to iron and steel, and elevated CSMR has been associated with galvanic corrosion of lead (Stets *et al.*, 2018).

The LR is calculated from the following expression (Stets *et al.*, 2018), where the concentrations of each species are expressed in mol/L:

$$LR = \frac{[Cl^-] + 2 * [SO_4^{2-}]}{[HCO_3^-]} \quad \textbf{(19)}$$

The CSMR is the mass ratio of chloride to sulphate (Stets *et al.*, 2018), where the concentrations of each species are expressed in mg/L:

$$CSMR = \frac{[Cl^-]}{[SO_4^{2-}]} \quad \textbf{(20)}$$

3 RESULTS AND DISCUSSION

3.1 IEX equilibria with increasing resin loading

The selectivity coefficients refer to the affinity of different ions for the resin and their estimation is key for the understanding of IEX equilibria (Crittenden *et al.*, 2012; SenGupta, 2017). In multicomponent systems (NOM, chloride, bicarbonate, sulphate and nitrate in this case), lower uptakes of ions of lower affinity can be observed than in pure binary systems because the counterions compete for the exchange sites (Boyer, Baird and Nirdosh, 1999). Similar selectivity coefficients were observed for the chloride-form (SO_4^{2-} > NOM > HCO_3^-> NO_3^-) and bicarbonate-form (SO_4^{2-} > NOM > NO_3^- ≈ Cl^-) resins with orders of selectivity (Table 1). The coefficients varied from 0.32-0.36 for nitrate to 2.53-2.84 for sulphate, with NOM having an intermediate selectivity of 0.51-0.57.

The order of selectivity follows the trend observed in the removal of each ion at equilibrium (Table S1) and are in most cases in line with published literature which predicts the influence of the degree of swelling within the resin and valence on the selectivity of the counterions (Crittenden *et al.*, 2012; SenGupta, 2017). The affinity for a given resin is dependent on the counterion charge and its size. Each ion has a hydrated radius composed of water molecules surrounding it, which becomes larger as the ionic radius decreases. These water molecules move together with the ion when it diffuses into the resin bead and consequently exert osmotic forces on the crosslinking bonds holding the resin matrix. Hence, the exchanger swells as the pores experience a swelling pressure caused by the resin elastic forces balancing the osmotic pressure gradient. Therefore, the ions with a larger ionic radius and higher charge are more preferably exchanged as they generate a lower resin swelling pressure (Crittenden *et al.*, 2012; SenGupta, 2017). Moreover, the electrostatic interactions taking place during IEX are known to be proportional to the valence of the counterions. Accordingly, the ions with higher charge (i.e. sulphate) exhibit greater affinity for the resin (Helfferich, 1995). Based on this and considering the ionic radii of the inorganic ions (258 pm for sulphate, 179 pm for nitrate, 172 pm for chloride and 156 pm for bicarbonate (Jenkins and Thakur, 1979)), the expected order of selectivity for the bicarbonate-form resin was SO_4^{2-} > NO_3^- ≈ Cl^-, which was similar to the

experimental results. For the chloride-form resin, the expected order of selectivity was SO_4^{2-} > NO_3^- > HCO_3^-, although the experimental results showed nitrate had slightly lower selectivity than bicarbonate by 0.13. The hydrated radii of nitrate and bicarbonate were very similar at 340 pm for nitrate (Volkov, Paula and Deamer, 1997) and 364 pm for bicarbonate (Kiss *et al.*, 2013). This explains their similar selectivity coefficients, particularly in a multicomponent system due to competition for the IEX sites. The selectivity of NOM, however, is difficult to determine due to the size distribution and molecular complexity of organic matter and is specific to each water source.

Table 1. Selectivity coefficients for chloride- and bicarbonate-form resin determined for a lowland river water source.

Anion	$K_{i\backslash Cl}$	$K_{i\backslash HCO3}$
Cl^-	1	0.37
SO_4^{2-}	2.53	2.84
NO_3^-	0.32	0.36
HCO_3^-	0.45	1
NOM (mg/L C)	0.51	0.57

When compared to results obtained for alternative resins, the selectivity established here was lower. To demonstrate, the selectivity coefficients for sulphate and nitrate towards MIEX resin in the chloride form were 4.34 and 1.26 respectively (Liu *et al.*, 2017), 1.7 and 3.9 times higher than those determined for the Lewatit S 5128 resin used in this study. The MIEX resin has a polyacrylic matrix similar to the Lewatit resin but has a macroporous structure. Although gel resins are characterised by a high adsorption capacity, macroporous resins allow for a better access of large ions to the active sites (SenGupta, 2017), which could explain the difference observed. For NOM, an increase in carboxylate chain length has been associated with an increase in selectivity with values ranging from 0.08 to 6.31 with the Amberlite IRA 458 resin (Cl-form), an acrylic gel type I SBA resin (Gregory and Semmens, 1972). Separation factors of 0.5 and 5.7 have been reported for NOM with a bicarbonate-form Purolite

A850 resin, a gellular type I SBA exchange resin in an acrylic matrix (Hu, Foster and Boyer, 2016), and for Suwannee River Fulvic Acid with a chloride-form MIEX resin (Boyer and Singer, 2008), respectively. The work of Croué *et al.* (1999) has shown that for Suwannee River NOM, the fractions that are characterized by higher molecular weights were associated with lower affinity for anion exchange resins. Indeed, for the resin and raw water used here, previous research has shown that low MW NOM fractions in the order of 1,000 g/mol and between 350-500 g/mol were particularly well removed, while higher MW NOM was less well removed (Finkbeiner et al., 2019; Fernandez et al., 2021a). These results highlight the complexity of estimating NOM selectivity due to the temporal and spatial variability of organic compounds found in drinking water sources.

Since the concept of selectivity describes the affinity of each species for the resin (Crittenden *et al.*, 2012) and the theoretical model applied in this research considers the electrostatic interactions as the mechanism taking place in the IEX process, one can expect that the selectivity should not be influenced by changes in the resin loading. Therefore, the selectivity coefficients previously determined were used as constants when modelling the IEX equilibrium after reusing the resin for 15 treatment cycles with no regeneration between cycles. The modelled data showed a good fit to the experimental data for the inorganic ions (Figure 1). This was shown by the small average difference between experimental and predicted concentrations of 0.11 mM (Table S2). The two IEX resin forms displayed similar performances over the 15 IEX treatment cycles for the inorganic ions (Figure 1). The presaturant ions, chloride and bicarbonate, showed a peak in concentration at cycle 1 (Figure 1) when the largest amounts of counterions were removed from the water (total of 5.8 and 4.9 meq/L respectively). The removal of nitrate and bicarbonate (for the chloride-form resin) or chloride (bicarbonate-form resin) stopped after cycle 4. Sulphate, however, continued to be removed up until cycle 12 (Figure 1) due to its higher selectivity for the resin (Table 1).

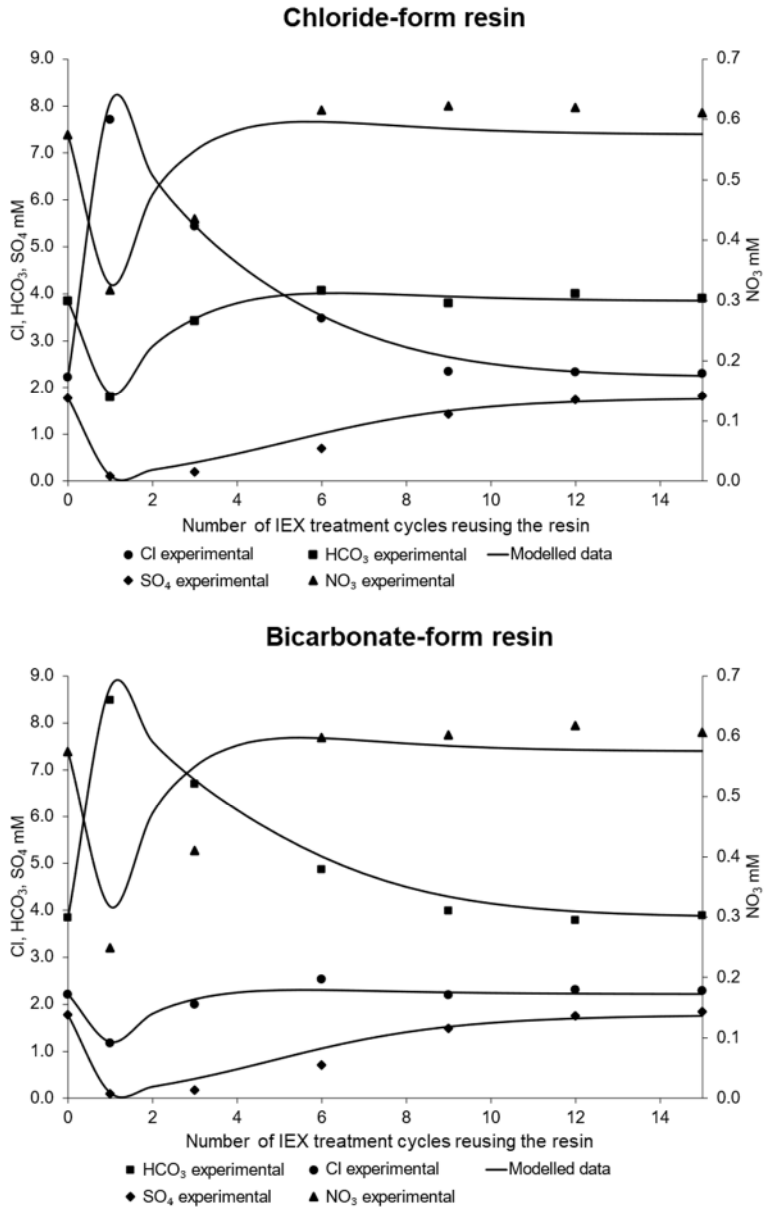


Figure 1. Experimental and modelled inorganic ion concentrations over 15 IEX jar tests reusing the resin and using constant selectivity coefficients forthe chloride- and bicarbonate-form resin.

As for NOM, subsequent removals were observed until cycle 15, with around 0.2 mM still being removed after cycle 9 with both resin forms (Figure 2). The model showed a good fit to the experimental data for both resin forms at cycle 1 (difference of 0.01 mM, Table S2) when using a constant selectivity coefficient (Figure 2). But a significant variation between the modelled and experimental data was noted for the following IEX treatment cycles, with an average difference of 0.21 mM (Table S2). Consequently, a

different approach was undertaken using a variable selectivity coefficient for NOM, based on the equilibrium theory and the experimental NOM concentrations after each treatment cycle (Figure 2). In this process, the calculated selectivity coefficients of the inorganic ions were kept constant. Text S2 shows the MATLAB script that was built for the iterative calculation process.

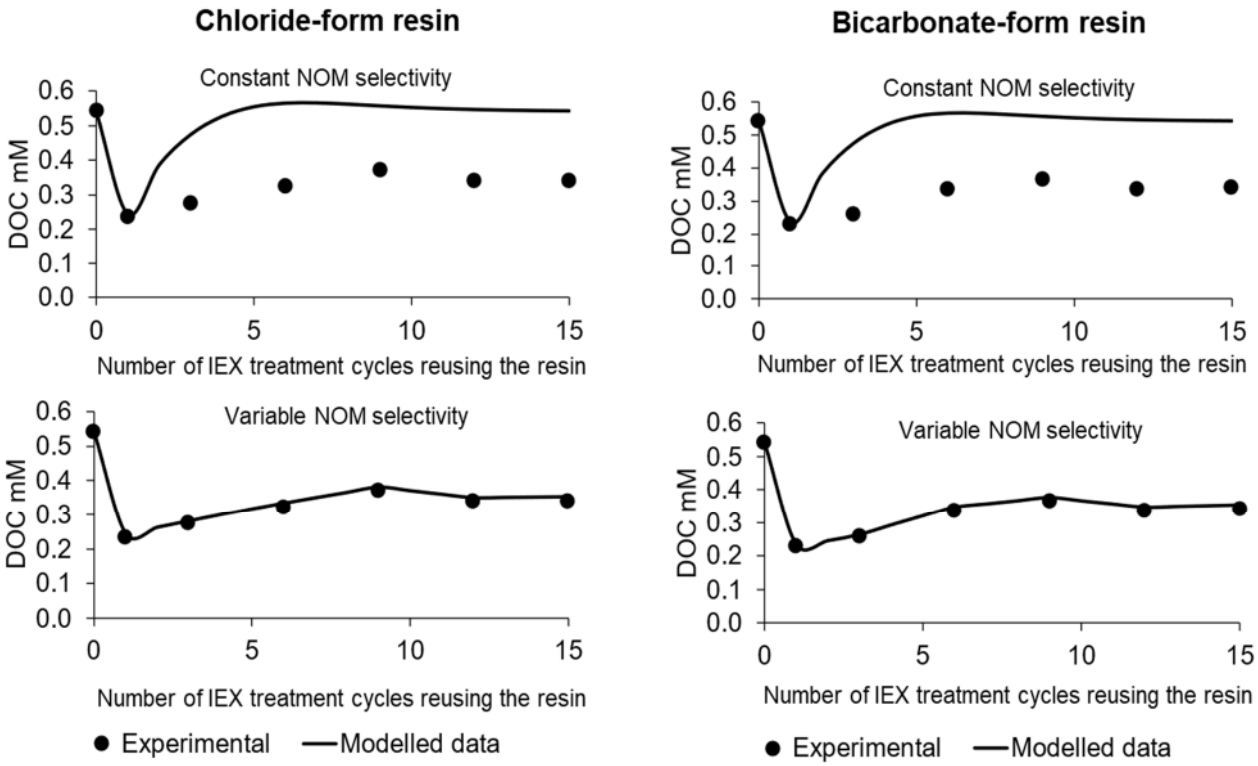


Figure 2. Experimental and modelled NOM concentrations (mM as DOC) reusing the chloride and bicarbonate resins for 15 IEX treatment cycles using constant (top) and variable (bottom) selectivity coefficients**.**

In this case, the model accurately fitted the experimental data as the average difference between predicted and measured NOM concentrations was reduced to 0.01 mM (Table S2). These results show that unlike the inorganic ions, the selectivity of the organic ions changes with the resin loading, supporting the idea that increases in resin loading impacts NOM but not the inorganic ions.

The variation in the selectivity coefficients of NOM showed a linear correlation with the number of treatment cycles ($R^2 > 0.99$) (Figure 3). The organic ions gradually became the most preferred ions for the resin as the affinity becomes higher than that of

sulphate after cycle 6. For example, from cycle 7 the selectivity of NOM was 2.9 and 3.1 for the chloride- and bicarbonate-form resins (Figure 3), while for sulphate it was 2.5 and 2.8, respectively (Figure 2).

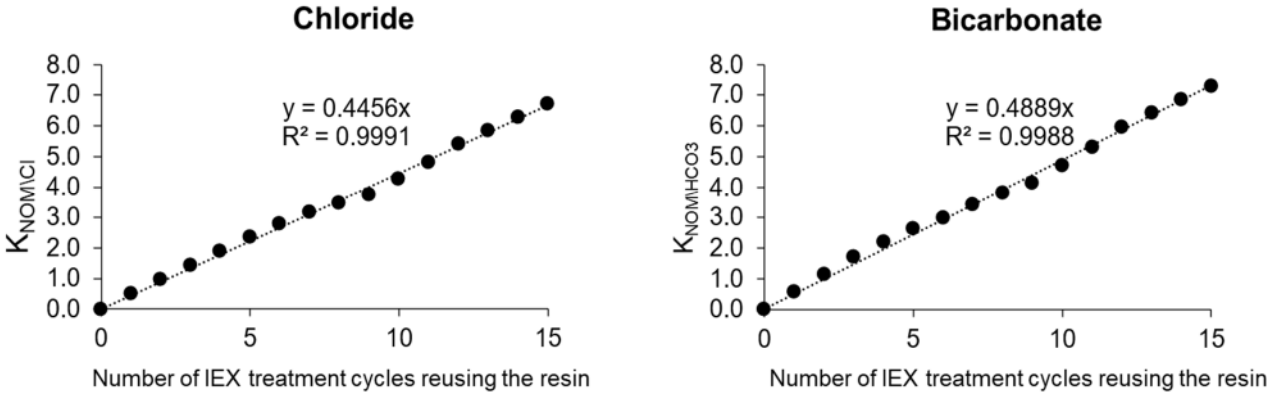


Figure 3. Variation in the selectivity coeficient for NOM reusing the resin over 15 IEX treatment cycles with the chloride- and bicarbonate-form resin

The prediction given by the IEX equilibrium model also allowed for the estimation of the resin loading over the 15 IEX treatment cycles (Figure 4). Accumulations of bicarbonate and nitrate, and chloride and nitrate could be observed up to cycle 3 for the chloride and bicarbonate-form resin, respectively, which was then followed by desorption of the same ions. This phenomenon has been reported by Edgar and Boyer (2021) and Fernandez (2021a) is referred to as secondary IEX, and is a consequence of the differences in affinity for the resin in multicomponent systems. Indeed, bicarbonate, chloride and nitrate have the smallest selectivity coefficients (Table 1), implying that these would exchange for the more preferred ions (sulphate and NOM) when the resin is not regenerated. As the selectivity of NOM increases, the model predicted a slight desorption of sulphate after cycle 12, with 0.34 and 0.36 mM desorbed between cycles 11 and 15 for the chloride and bicarbonate-form resin respectively. Additionally, the model showed that the increased NOM loading in the resin followed a linear trend as the resin was reused for 15 cycles, showing that a constant amount of NOM (0.22 mM) was adsorbed during each cycle (Figure S3). The continued adsorption of NOM without regenerating the resin was a consequence of secondary IEX, where inorganic ions already adsorbed on the resin from previous

cycles (i.e. nitrate) exchange with NOM instead of the initial presaturant (either chloride or bicarbonate).

The model was subsequently used to predict resin loading during long-term use without regeneration, considering up to 1000 cycles (equivalent to 21 days of continuous operation without regeneration at a 30 min retention time) (Figure 4). The model predicted that the secondary IEX observed would continue until NOM occupied nearly all of the sites (98%) at cycle 1000, assuming the water quality did not change. Indeed, while NOM continues to be adsorbed, all the other ions present on the resin start desorbing at different cycles depending on their affinity for the resin. Therefore, when the resin is close to NOM saturation at cycle 1000, its removal ceases.

The proposed IEX multicomponent model provides a good fit to experimental data and can be recalibrated for other water sources and other polyacrylic resins.

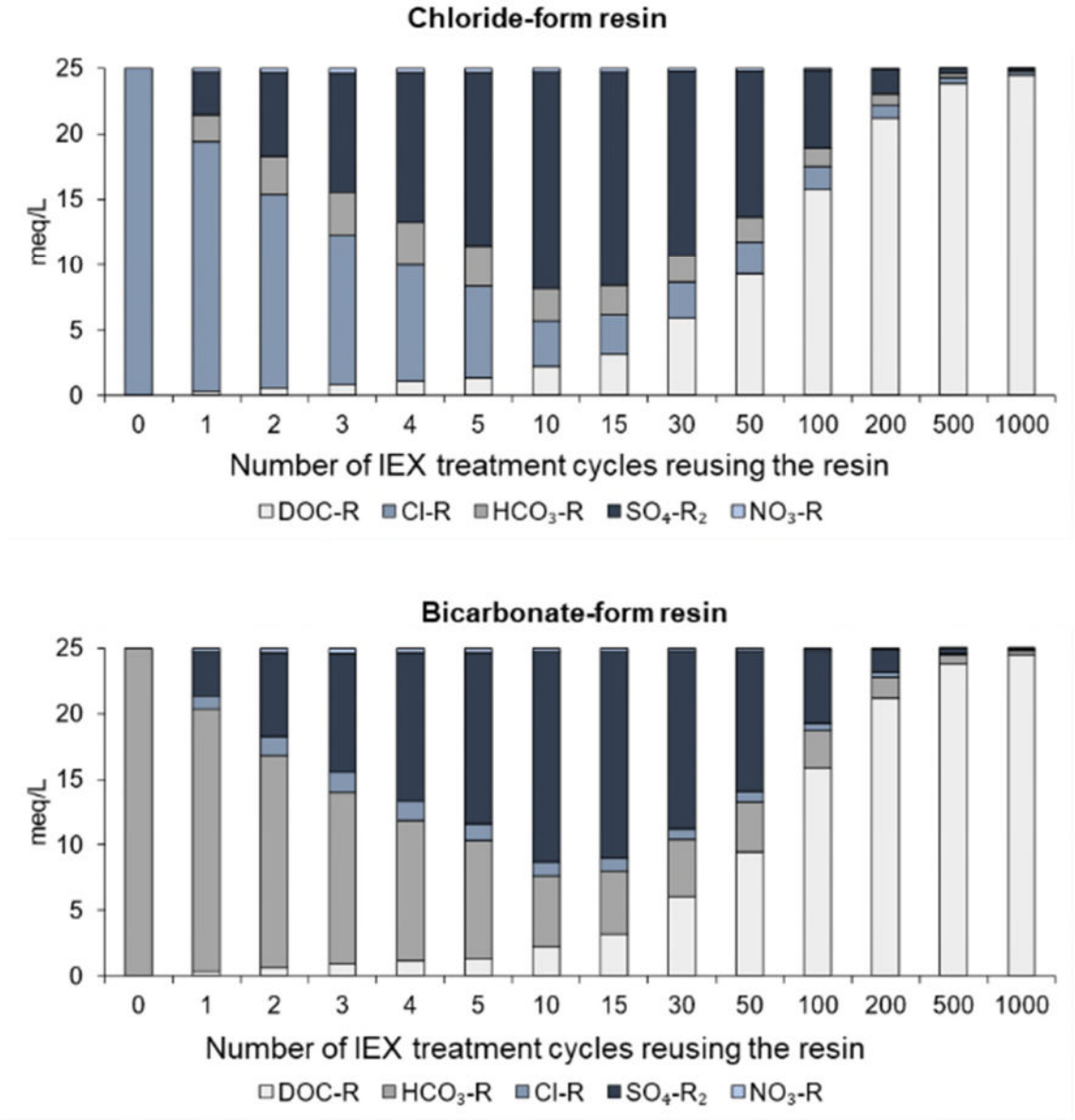


Figure 4. Modelled composition of the chloride- and bicarbonate-form resin loading over 1000 IEX treatment cycles

The IEX equilibrium model accounts for electrostatic interactions and, as a result, has been built to maintain electroneutrality within the system over non-regenerated cycles. However, the experimental data revealed that the resin loading (total milliequivalents present on the resin) was higher than the apparent meq capacity of the resin (Figure 5). Indeed, the total of the ion charge removed exceeded the initial exchange capacity by a maximum of 7.4 and 8.2 meq/L for the chloride and bicarbonate-form resin respectively, with a plateau being observed after cycle 12. The experimental findings

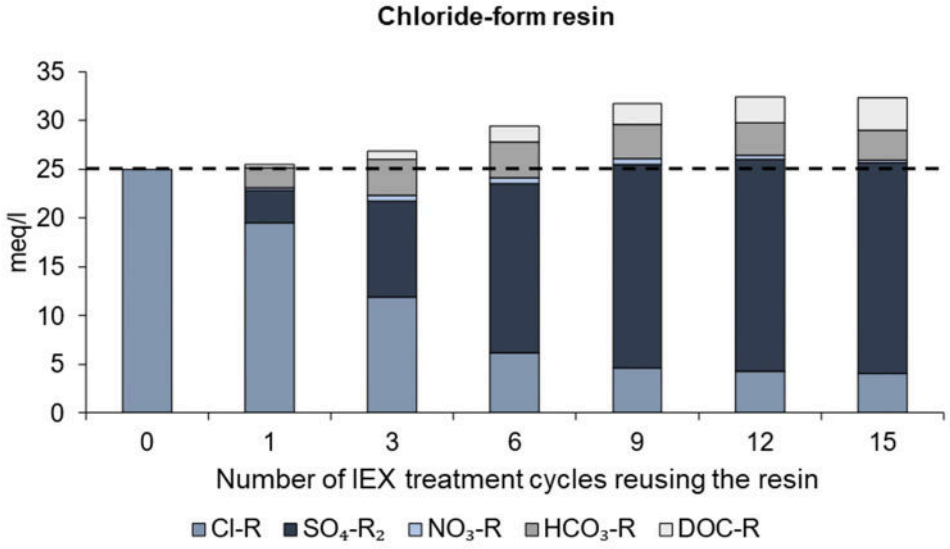
and the results derived from the model support the view of multiple NOM molecules being removed per exchange site.

Previous research has reported on hydrophobic interactions between resin and adsorbed NOM (SenGupta, 2017). However, because of the hydrophilic structure of the polyacrylic resin used in this study, hydrophobic interactions can be considered negligible (Shuang et al., 2015). Therefore, different mechanisms for the increased capacity in this study must be considered. Previous research supports the theory of an admicelle (micelle bilayer) formation by humic acids on the IEX acrylic resin surface when reused without regeneration (Asnachinda *et al.*, 2010; Eastoe and Tabor, 2014). Moreover, it has been reported that organic molecules can access the hydrophobic regions of the admicelle through adsolubilisation, which favours their diffusion into the resin gel matrix, while the admicelle acts as a barrier to other anions (Cheng and Sabatini, 2002; Cheah, 2016). Shuang *et al.* (2015) also suggested that micelle-based clusters of humic acids may form on polyacrylic resins.

NOM in this water source was characterised through liquid chromatography with organic carbon detection (LC-OCD) (Figure S1). The analysis indicated that dominant fraction was at the molecular size 1000 g/mol, which has been associated with humic-like substances (Huber *et al.*, 2011). Amongst these, humic acids are relatively hydrophobic and are typically preferred by quaternary ammonium functional groups (SenGupta, 2017). They also present an amphiphilic structure that enables them to function as natural surfactants (Guetzloff and Rice, 1994; Ctvrtnickova *et al.*, 2011) and allow for the formation of admicelles (Cheng and Sabatini, 2002; Cheah, 2016). This could explain the additional milliequivalents observed in the resin phase over its original capacity. Consequently, two mechanisms appear to be taking place for organic matter removal: electrostatic interaction and physical adsorption. However, confirmation of this hypothesis should be performed by determining the molecules adsorbed on the resin over increasing load or using model compounds in future research.

The model has highlighted the different mechanisms of NOM removal during IEX. However, it is worth noting that the model is limited in its capacity to fully represent these mechanisms. The variable selectivity coefficients of NOM determined in this

study are the values needed to match the experimental NOM concentrations when the electrostatic interactions are the sole mechanism taking place. Figure S2 indicates that sulphate desorbed at cycle 15 for both resin forms rather than cycle 12 as predicted by the model. Thus, the contribution of the electrostatic interactions may be overestimated in this model and the contribution of physical adsorption underestimated. Consequently, the increase in the selectivity of NOM could be different from that seen over the 15 experimental cycles. For instance, sulphate might not fully desorb and multilayers of humic acid micelles may be formed on the resin surface (Eastoe and Tabor, 2014).



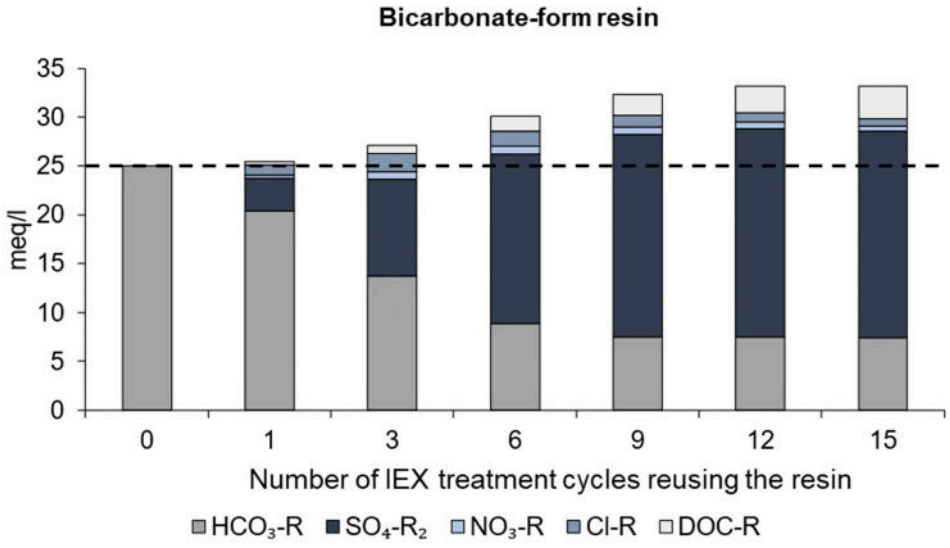


Figure 5. Composition of the chloride- and bicarbonate-form resin determined experimentally reusing the resin for 15 IEX jar tests. The dotted line indicates the capacity of the resin.

The model was used to estimate the regeneration of a saturated resin at different regeneration frequencies (from every treatment cycle to 15 reuse cycles) and increasing resin loading (Figure 6). Similarly to the modelling of the ion concentrations in the aqueous phase at equilibrium (Figures 1 and 2), the selectivity of NOM was varied and the selectivity of the inorganic ions was kept constant.

It was observed that the initial chloride and bicarbonate resin-phase concentrations of 25 meq/L was almost fully recovered up to cycle 10. However, as the regeneration frequency decreased, the model estimated that some of the ions would not desorb from the resin. For example, when pushed beyond the 15 experimental cycles to 1000 cycles, the model predicted 18.5 meq/L of other ions still present on the resin. The use of higher chloride or bicarbonate concentrations could be considered to improve the efficiency of the regeneration. Indeed, higher concentration gradients increase the amounts of contaminants exchanged as the system reaches equilibrium (SenGupta, 2017).

The regeneration method investigated is commonly performed with a contact time of 30 min. However, as the accumulation of anion contaminants on the resin increases, a longer contact time might be needed to reach the equilibrium state. Moreover, high retention times promote the deep diffusion of NOM inside the resin pores (Mergen, 2008). This, and the association of NOM, increase the risk of irreversible fouling as organic compounds might not fully desorb during regeneration (SenGupta, 2017). Although some authors have reported better resistance of polyacrylic resins to fouling than polystyrene resins (Harland, 1994; Shuang *et al.*, 2015), there is a need to develop long-term experimental information to assess these risks at lower regeneration frequency.

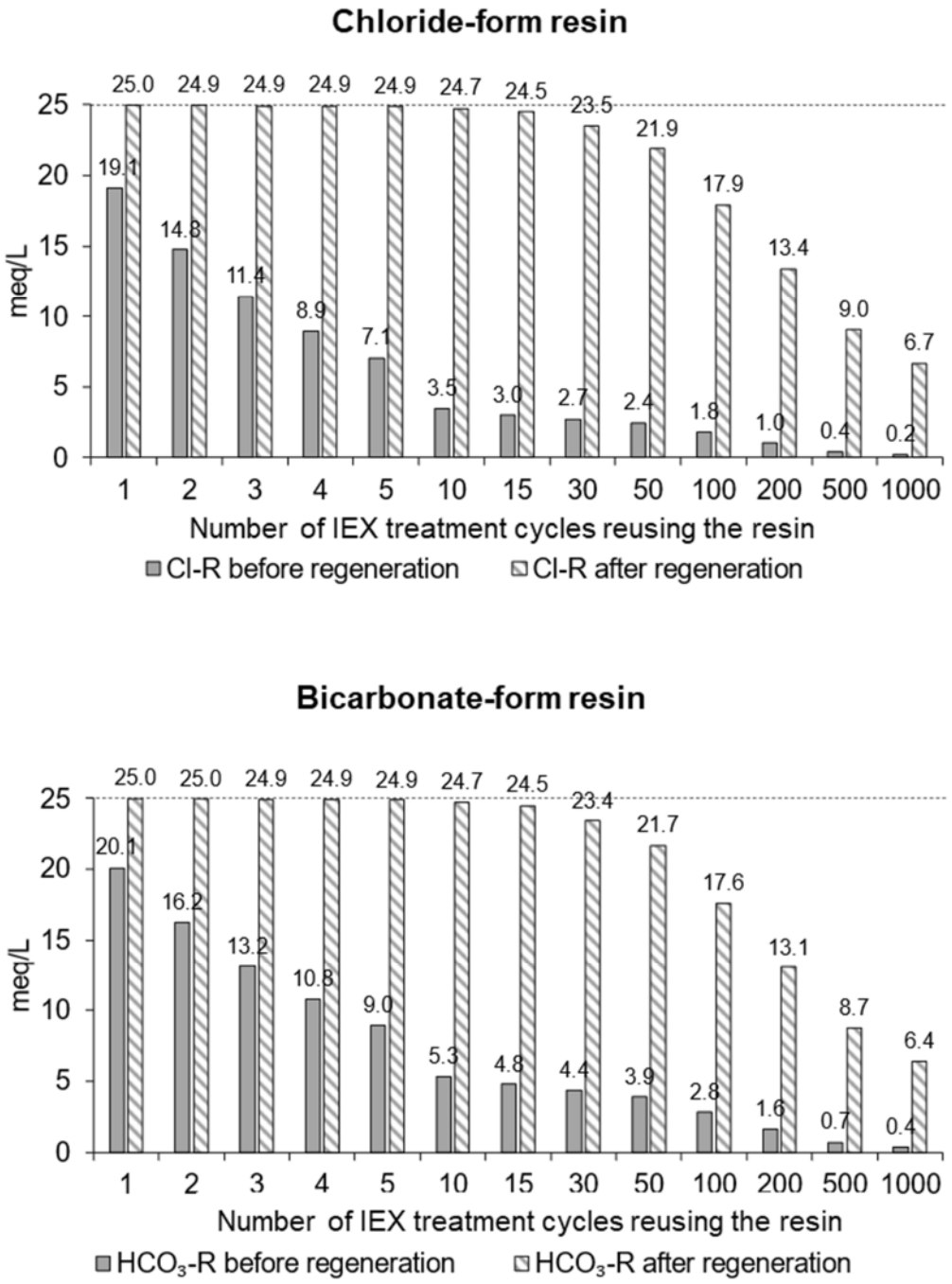


Figure 6. Resin regeneration with 1 M chloride and bicarbonate brine after reusing the resin between 1 and 1000 IEX treatment cycles.

3.2 Implications of operating IEX under reduced regeneration frequencies

Operating IEX under suboptimal regeneration frequencies (not regenerating the resin every treatment cycle) can result in lower brine use and waste generation. However, it may have a negative impact on NOM removal due to the increased resin loading while also affecting the treated water quality and corrosivity. To assess the implications of increased resin loading during reduced regeneration frequency, four scenarios were investigated, where resin regeneration was performed either every IEX treatment cycle, every 5 cycles, 15 cycles or 20 cycles. Under these scenarios NOM removal was 56%, 41%, 35% and 35%, respectively, based on the experimental data and the model (Figures 2 and 4). NOM removal when the resin was regenerated every 15 or 20 treatment cycles was the same since reusing the resin more than 12 times did not change NOM removal (Figure 2).

Although the selectivity of NOM increases, its removal decreases due to the accumulation of the most preferred ions on the resin over treatment cycles during secondary IEX (Figure 4). Indeed, as the resin is reused without regeneration, the removal of NOM becomes more difficult as NOM exchanges with ions that have a higher selectivity for the resin compared to chloride or bicarbonate (i.e., sulphate). Therefore, the competition for the resin active sites increases and the removal of NOM will be lower with a used resin than for a resin initially saturated with one regenerant. This has a direct impact on the treated water corrosivity as it is affected by the concentration of chloride and sulphate. This is shown by the LR and CSMR indexes (Figure 7). LR < 0.8 indicates a low corrosion rate in iron and steel pipes, 0.8 < LR < 1.2 a moderate corrosion, and LR > 1.2 a high corrosion rate (Lytle *et al.*,2020); and CSMR > 0.5 increase the risk of galvanic corrosion of leaded connections (Stets *et al.*, 2018).

When regenerating every treatment cycle, the use of bicarbonate reduced the LR and CSMR from 4.5 and 25.5 with chloride to 0.2 and 4.0 respectively. However, because of the secondary IEX taking place, the aqueous-phase concentrations of sulphate increase, while the aqueous-phase concentrations of bicarbonate decrease over treatment cycles without regeneration (Figure 1). Therefore, there is an increase in the

LR by 0.5 and 0.8 after 5 and 15 cycles for the bicarbonate-form resin until reaching the LR values obtained for chloride (Figure 7). As for the CSMR, lower values were obtained with bicarbonate when reusing the resin 1 and 5 times (4 and 0.9 vs 25 and 1.7, respectively). Reusing the resin 15 and 20 cycles resulted in similar values for both resin forms due to secondary IEX. Based on these results, and from a corrosivity point of view, reusing the resin every 5 treatment cycles and using the bicarbonate-form resin was the condition that ensured water corrosivity is kept within acceptable limits.

The volumes of brine used and waste generated were estimated under these conditions (Figure 7). Compared to a regeneration frequency every treatment cycle, the brine and waste volumes per volume of treated water decreased by 79%, 92% and 94% for a regeneration frequency of 5, 15 and 20 cycles, respectively.

Results showed that there is a balance between corrosivity, brine usage, waste production and NOM removal, where the bicarbonate-form resin performed similarly in terms of NOM removal to the chloride-form resin but offered the potential for lower corrosivity. Whilst working under regeneration frequencies of 15 and 20 cycles can reduce the brine and waste more than 90%, the treated water quality is lower. In particular, the risk of corrosivity shown by the LR index is twice as high as when regenerating the resin every 5 cycles. IEX treatment of this source water reusing the bicarbonate-form resin every 5 cycles would achieve the most sustainable balance. The data showed a NOM removal of 41%, LR and CSMR values of 0.7 and 0.9, respectively, and 79% reduction in brine and waste volumes. The model also showed that for this regeneration frequency, almost 100% of the exchange capacity was recovered after regeneration (Figure 6). Operating IEX under resin regeneration frequencies between 1 and 5 treatment cycles should be based on NOM removal requirements. While reusing the resin 5 times reduces waste and brine in comparison to optimal regeneration, it also reduced NOM removal by 15%. However, as previously highlighted, further work is needed to account for the admicelle formation and irreversible fouling in the model, as well as to assess long-term regeneration efficiency. For instance, the exchange capacity recovery could be less than that predicted at long regeneration frequencies and higher volumes of brine and waste could be required.

These results highlight the water quality and environmental benefit of operating at reduced regeneration frequency, which can be quantified as long as the resin loading is characterised.

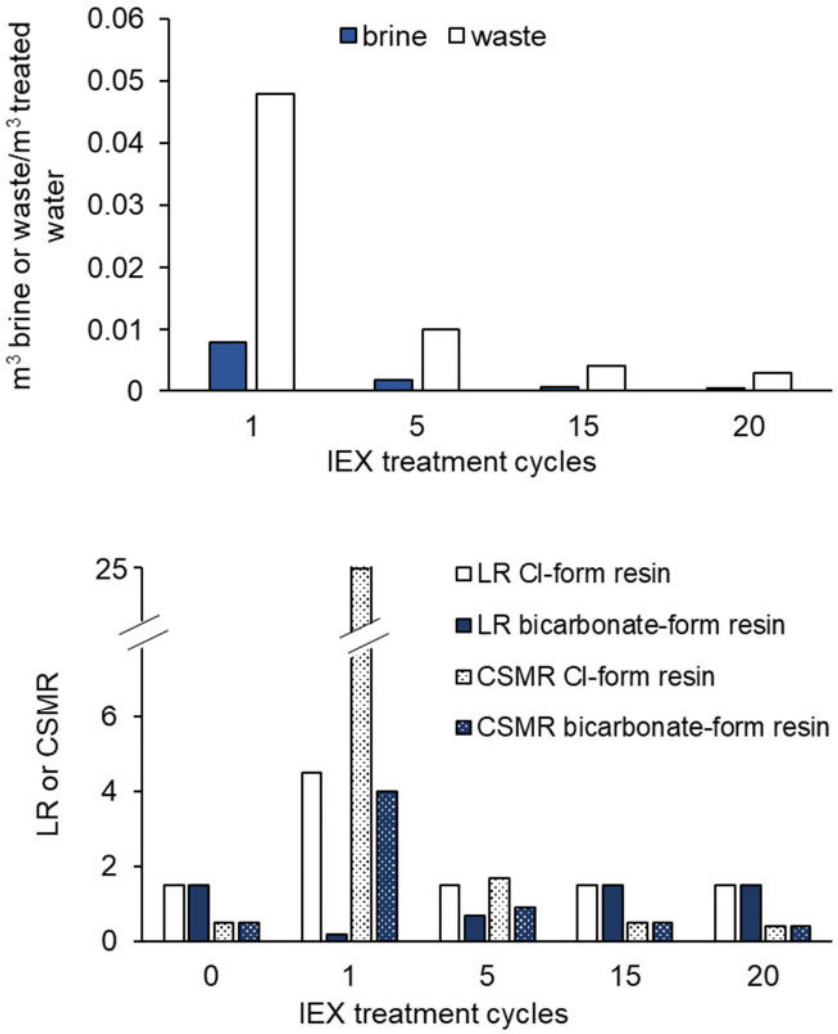


Figure 7. Brine and waste produced per volume of treated water and LR and CSMR corrosivity indexes in the raw water and after IEX treatment when the resin has been reused 1, 5, 15 or 20 treatment cycles.

4. CONCLUSIONS

An IEX equilibrium model that considers changes in the resin loading during reduced regeneration was developed and was able to account for increases in resin loading in both the chloride- and bicarbonate-form resin. The model contributed to the

understanding of the adsorption mechanisms and showed that contrarily to inorganic ions, the selectivity of NOM increased with resin loading. It also showed that the initial capacity of the resin was exceeded. This suggested that two mechanisms are taking place for NOM removal - electrostatic interactions and admicelle formation.

The model was used to assess the implications of reduced regeneration frequency on the operation of IEX process treatment. Results revealed that under reduced regeneration frequencies, brine use and waste generation can be reduced by more than 90%, where the bicarbonate-form resin performed similarly in terms of NOM removal to the chloride-form resin but offered the potential for lower corrosivity. However, changes in resin loading due to secondary IEX showed that the risk of corrosion increases when the resin is bicarbonate-form reused more than 5 times. For the tested source water, reusing the bicarbonate-form resin every 5 cycles would achieve the most balanced option with 41% NOM and 79% reduction in brine and waste volumes. The model showed that under these conditions, almost 100% of exchange capacity is recovered after regeneration. These results highlight the water quality and environmental benefit of operating at reduced regeneration frequency, which can be quantified as long as the resin loading is characterised.

Further research is required to include the contributions of the electrostatic interactions and physical adsorption behind NOM removal. The model should be adapted to account for potential losses in exchange capacity at reduced regeneration frequency. Although the model can be recalibrated to other water sources and other acrylic resins, more detailed NOM characterisation such as molecular size and structure should be incorporated in the model to identify trends in selectivity that would allow the application of the model to any water source.

ACKNOWLEDGMENTS

The Authors would like to acknowledge Anglian Water Services, UK, for supporting this research.

REFERENCES

Asnachinda, E., O'Haver, J. H., Sabatini, D. A. and Khaodhiar, S. (2010) 'Atomic force microscopy and contact angle studies of polymerizable gemini surfactant admicelles on mica', *Journal of Applied Polymer Science*. John Wiley & Sons, Ltd, 115(2), pp. 1145–1152. doi: 10.1002/APP.31224.

Boyer, W. D. A., Baird, M. H. I. and Nirdosh, I. (1999) 'Ion exchange equilibria in binary and ternary systems', *The Canadian Journal of Chemical Engineering*. John Wiley & Sons, Ltd, 77(1), pp. 92–98. doi: 10.1002/CJCE.5450770115.

Boyer, T. H. and Singer, P. C. (2008) 'Stoichiometry of removal of natural organic matter by ion exchange', Environmental Science and Technology. American Chemical Society, 42(2), pp. 608–613. doi: 10.1021/es071940n.

Carra, I., Fernandez Lozano, J., Johannesen, S., Godart-Brown, M., Goslan, E. H., Jarvis, P. and Judd, S. (2021) 'Sorptive removal of disinfection by-product precursors from UK lowland surface waters: Impact of molecular weight and bromide', *Science of The Total Environment*, 754, pp. 142–152. doi: https://doi.org/10.1016/j.scitotenv.2020.142152.

Cheah, P. L. (2016) *Investigation Of Parameters Enabling Admicellar Reversible Addition-Fragmentation Chain Transfer (Raft) Polymerization*, PhD Thesis, *University of Mississippi*.

Cheng, H. and Sabatini, D. (2002) 'Simultaneous uptake of anionic surfactants and micellar-solubilized contaminants using anion-exchange resins', *Water research*. Water Res, 36(8), pp. 2062–2076. doi: 10.1016/S0043-1354(01)00411-0.

Crittenden, J. C., Trussell, R. R., Hand, D. W., Howe, K. J. and Tchobanoglous, G. (2012) *MWH´s Water Treatment Principles and Design*.

Croué, J. P., Violleau, D., Bodaire, C. and Legube, B. (1999) 'Removal of hydrophobic and hydrophilic constituents by anion exchange resin', *Water Science and Technology*. IWA Publishing, 40(9), pp. 207–214. doi: 10.1016/S0273-1223(99)00658-7.

Ctvrtnickova, A. U., Drastík, M., David, J. and Kucerik, J. (2011) ‘Surface and solution behavior of surfactants produced from lignite humic acids’, *Fresenius Environmental Bulletin*, 20(7A), pp. 1764–1771.

Dranoff, J. and Lapidus, L. (1957) ‘Equilibrium in Ternary Ion Exchange Systems’, *Industrial and Engineering Chemistry*, 49(8), pp. 1297–1302. doi: 10.1021/ie50572a038.

Eastoe, J. and Tabor, R. F. (2014) ‘Surfactants and Nanoscience’, *Colloidal Foundations of Nanoscience*. JAI-Elsevier Science Inc, pp. 135–157. doi: 10.1016/B978-0-444-59541-6.00006-0.

Edgar, M. and Boyer, T. (2021) ‘Removal of natural organic matter by ion exchange: Comparing regenerated and non-regenerated columns’, *Water research*. Water Res, 189. doi: 10.1016/J.WATRES.2020.116661.

Fernandez, J., Dunn, C., Brookes, A., Jarvis, P. and Carra, I. (2021a) 'Feasibility Study of Suspended Ion Exchange for Organic Matter Removal and Disinfection By-product Minimisation in UK Lowland Waters', *Institute of Water* Journal, 6, pp 4-10.

Fernandez, J., Jarvis, P., Brookes, A., Knott, S. and Carra, I. (2021b) 'Impact of Bicarbonate as Regenerant and Resin Age on Organic Matter Removal, Disinfection By-product Formation and Adsorption Mechanisms*', Journal of Water Process Engineering,* 44, pp. 102337. https://doi.org/10.1016/j.jwpe.2021.102337

Finkbeiner, P., Moore, G., Tseka, T., Nkambule, T. T. I., Kock, L. De, Jefferson, B. and Jarvis, P. (2019) ‘Interactions between Organic Model Compounds and Ion Exchange Resins’, *Environmental Science and Technology*, 53(16), pp. 9734–9743. doi: 10.1021/acs.est.9b02139.

Galjaard, G., Koreman, E., Metcalfe, D., Moore, G. and Ericsson, P. (2018) ‘NOM-removal by the SIX®-process’, *Water Practice and Technology*, 13(3), pp. 524–541. doi: 10.2166/WPT.2018.072.

Gregory, J. and Semmens, M. J. (1972) ‘Sorption of carboxylate ions by strongly basic anion exchangers’, *Journal of the Chemical Society, Faraday Transactions 1: Physical Chemistry in Condensed Phases*. The Royal Society of Chemistry, 68(0), pp. 1045–

1052. doi: 10.1039/F19726801045.

Guetzloff, T. F. and Rice, J. A. (1994) 'Does humic acid form a micelle?', *Science of The Total Environment*. Elsevier, 152(1), pp. 31–35. doi: 10.1016/0048-9697(94)90548-7.

Hannachi, C., Guesmi, F. and Hamrouni, B. (2013) 'Study of the ion exchange equilibrium of Cl-, NO3-, and SO42- ions on the AMX membrane', *Ionics*, 19(2), pp. 329–334. doi: 10.1007/S11581-012-0740-X.

Harland, C. E. (1994) *Ion Exchange*. Cambridge: The Royal Society of Chemistry (RSC Paperbacks). doi: 10.1039/9781847551184.

Helfferich, F. G. (1995) *Ion exchange*. Dover Publications Inc.

Hu, Y., Foster, J. and Boyer, T. H. (2016) 'Selectivity of bicarbonate-form anion exchange for drinking water contaminants: Influence of resin properties', Separation and Purification Technology. Elsevier, 163, pp. 128–139. doi: 10.1016/J.SEPPUR.2016.02.030.

Huber, S. A., Balz, A., Abert, M. and Pronk, W. (2011) 'Characterisation of aquatic humic and non-humic matter with size-exclusion chromatography – organic carbon detection – organic nitrogen detection (LC-OCD-OND)', *Water Research*. Elsevier, 45(2), pp. 879–885. doi: 10.1016/J.WATRES.2010.09.023.

Jenkins, H. D. B. and Thakur, K. P. (1979) 'Reappraisal of thermochemical radii for complex ions', Journal of Chemical Education, 56, 9, 576. https://doi.org/10.1021/ed056p576

Kiss, A. M., Myles, T. D., Grew, K. N., Peracchio, A. A., Nelson, G. J. and Chiu, W. K. S. (2013) 'Carbonate and Bicarbonate Ion Transport in Alkaline Anion Exchange Membranes', *Journal of The Electrochemical Society*. IOP Publishing, 160(9), pp. F994–F999. doi: 10.1149/2.037309JES.

Lenntech (2016) *Product Information Lewatit ® s 5128*.

Liu, C., Zhu, L., Zhang, Q. and Chen, W. (2017) 'Preparation of nitrate-selective porous magnetic resin and assessment of its performance in removing nitrate from

groundwater', *Environmental technology*. Taylor & Francis Group, LLC, 38(3), pp. 231–238. doi: 10.1080/09593330.2016.1189970.

Lytle, D. A., Tang, M., Francis, A. T., O'Donnell, A. J. and Newton, J. L. (2020) 'The effect of chloride, sulfate and dissolved inorganic carbon on iron release from cast iron', *Water Research*. Elsevier, 183. doi: 10.1016/J.WATRES.2020.116037.

Mergen, M. R. D. (2008) *Impact of magnetic resin on DOC removal and downstream water treatment processes*. Cranfield University.

Nguyen, C. K., Clark, B. N., Stone, K. R. and Edwards, M. A. (2011) 'Role of Chloride, Sulfate, and Alkalinity on Galvanic Lead Corrosion', *Corrosion*. Allen Press, 67(6), pp. 065005–1–065005–9. doi: 10.5006/1.3600449.

PWN Technologies (2017) *Technical White Paper SIX ® Technology by PWN Technologies*.

Rokicki, C. A. and Boyer, T. H. (2011) 'Bicarbonate-form anion exchange: affinity, regeneration, and stoichiometry', *Water research*. Elsevier, 45(3), pp. 1329–1337. doi: 10.1016/J.WATRES.2010.10.018.

Semmens, M. J., Burckhardt, M., Schuler, D., Davich, P., Slunjski, M., Bourke, M. and Nguyen, H. (2000) 'An evaluation of magnetic ion exchange (MIEX®) for NOM removal', in *AWWA Conference*. Denver, USA.

SenGupta, A. K. (2017) *Ion Exchange in Environmental Processes*: *Fundamentals, Applications and Sustainable Technology*. John Wiley & Sons, Inc. doi: 10.1002/9781119421252.

Shuang, C., Wang, J., Li, H., Li, A. and Zhou, Q. (2015) 'Effect of the chemical structure of anion exchange resin on the adsorption of humic acid: Behavior and mechanism', *Journal of Colloid and Interface Science*. Elsevier, 437, pp. 163–169. doi: 10.1016/J.JCIS.2014.09.011.

Stets, E. G., Lee, C. J., Lytle, D. A. and Schock, M. R. (2018) 'Increasing chloride in rivers of the conterminous U.S. and linkages to potential corrosivity and lead action level exceedances in drinking water', *The Science of the total environment*. Elsevier,

613–614, pp. 1498–1509. doi: 10.1016/J.SCITOTENV.2017.07.119.

Tang, M., Nystrom, V., Pieper, K., Parks, J., Little, B., Guilliams, R., Esqueda, T. and Edwards, M. (2018) 'The Relationship Between Discolored Water from Corrosion of Old Iron Pipe and Source Water Conditions', *Environmental Engineering Science*. Mary Ann Liebert, Inc., 35(9), pp. 943–952. doi: 10.1089/EES.2017.0435.

Volkov, A. G., Paula, S., Deamer, D. W. (1997). ' Two mechanisms of permeation of small neutral molecules and hydrated ions across phospholipid bilayers', *Bioelectrochemistry and Bioenergetics, 42, pp 153-160/ https://doi.org/10.1016/S0302-4598(96)05097-0*

Zhang, H., Shields, A. J., Jadbabaei, N., Nelson, M., Pan, B. and Suri, R. P. S. (2014) 'Understanding and Modeling Removal of Anionic Organic Contaminants (AOCs) by Anion Exchange Resins', *Environmental Science and Technology*. American Chemical Society, 48(13), pp. 7494–7502. doi: 10.1021/ES500914Q.



https://dspace.org/

Impact of resin loading on ion exchange equilibrium for removal of organic matter and inorganic ions

Pidoux, Lucie; Shorney-Darby, Holly; Vaudevire, Elisabeth; Martijn, Bram; Jarvis, Peter ...

2022-02-19
Elsevier
https://doi.org/10.1016/j.jhazmat.2022.128530
Pidoux L, Shorney-Darby H, Vaudevire E, et al., (2022) Impact of resin loading on ion exchange equilibrium for removal of organic matter and inorganic ions. Journal of Hazardous Materials, Volume 431, June 2022, Article number 128530

Downloaded from a DSpace repository. https://dspace.org/